

# Open Research Online

---

The Open University's repository of research publications and other research outputs

## Mitigating Cutting-Induced Plasticity Errors in the Determination of Residual Stress at Cold Expanded Holes Using the Contour Method

### Journal Item

#### How to cite:

Kim, H.K.; Carlson, S. S.; Stanfield, M. L.; Paddea, Sanjooram; Hosseinzadeh, F. and Bouchard, P. J. (2022). Mitigating Cutting-Induced Plasticity Errors in the Determination of Residual Stress at Cold Expanded Holes Using the Contour Method. *Experimental Mechanics*, 62 pp. 3–18.

For guidance on citations see [FAQs](#).

© 2021 H.K. Kim et al.



<https://creativecommons.org/licenses/by/4.0/>

Version: Version of Record

Link(s) to article on publisher's website:

<http://dx.doi.org/doi:10.1007/s11340-021-00756-z>

---

Copyright and Moral Rights for the articles on this site are retained by the individual authors and/or other copyright owners. For more information on Open Research Online's data [policy](#) on reuse of materials please consult the policies page.

---

[oro.open.ac.uk](http://oro.open.ac.uk)



# Mitigating Cutting-Induced Plasticity Errors in the Determination of Residual Stress at Cold Expanded Holes Using the Contour Method

H. K. Kim<sup>1</sup> · S. S. Carlson<sup>2</sup> · M. L. Stanfield<sup>2</sup> · S. Paddea<sup>3</sup> · F. Hosseinzadeh<sup>1</sup> · P. J. Bouchard<sup>1</sup>

Received: 9 March 2021 / Accepted: 8 July 2021  
© The Author(s) 2021

## Abstract

**Background** The split sleeve cold expansion process is widely used to improve the fatigue life of fastener holes in the civil and military aircraft industry. The process introduces beneficial compressive residual stresses around the processed hole, but uncertainties remain about the character of the stress field immediately adjacent to the bore of the hole.

**Objective** The primary objective of this study was to implement the contour method with minimising error associated with cutting-induced plasticity to provide detailed and reliable characterisation of the residual stress introduced by the split sleeve cold expansion process.

**Methods** A systematic FE study of plasticity effects by simulating different contour cutting strategies (a single cut, two sequential cuts and a 6-cut sequence) for a cold expanded hole in an aluminium alloy coupon was conducted. The identified ‘optimum’ cutting strategy was then applied experimentally on coupons containing a hole that had been processed to 3.16% applied expansion.

**Results** The FE study of different cutting simulations show that the locations of the stress error is consistent with the location where cutting-induced plasticity accumulated and that the magnitude and locations of stress re-distribution plasticity can be controlled by an optimised cutting strategy. In order to validate this hypothesis a high quality contour measurement was performed, showing that accurate near bore stress results can be achieved by the proposed 6-cut approach that controls cutting induced plasticity.

**Conclusions** The present work has demonstrated that detailed FE simulation analysis can be a very effective tool in supporting the development of an optimum cutting sequence and in making correct choices of boundary conditions. Through optimizing these key aspects of the cutting sequence one is much more likely to have a successful, low error contour residual stress result.

## Introduction

Fastener holes are essential in aircraft structures to allow for the mating of structural items. The introduction of a fastener hole into a critical structural member introduces a local stress concentration under far field operational loading. These geometric notches are therefore susceptible to fatigue nucleation and subsequent crack propagation, requiring regular in-service inspection to

be performed in order to maintain the structural integrity of an operational fleet. In an effort to increase the length of time before an initial inspection, and between recurring inspections, the Split Sleeve Cold Expansion<sup>TM</sup> (SSCx<sup>TM</sup>) process was developed in the early 1970s by the Boeing Company, then later patented and marketed by Fatigue Technology Incorporation (FTI) [1, 2]. The process introduces a deep residual compressive stress in the material around the processed fastener hole. This local compressive residual stress is balanced by a far field low-level tensile stress. The SSCx<sup>TM</sup> process is performed by hydraulically pulling a tapered mandrel through a lubricated sleeve which has been placed between the mandrel and the fastener hole. It has been demonstrated repeatedly that this process increases the fatigue crack growth life of treated fastener holes [2–4]. However, the magnitude and distribution of the residual stress developed by the SSCx<sup>TM</sup> process is complex owing to many factors such

✉ H. K. Kim  
ho.kim@open.ac.uk

<sup>1</sup> School of Engineering & Innovation, The Open University, Milton Keynes MK7 6AA, UK

<sup>2</sup> Southwest Research Institute (SwRI), 6220 Culebra Rd, San Antonio TX 78238, USA

<sup>3</sup> Stress-Space Ltd, Atlas Building, Harwell Campus, Didcot OX11 0QX, UK



as imperfect axisymmetry, variations through the thickness due to the mandrel being pulled through the material, cyclic material properties and the initial hole diameter [5]. But for accurate prediction of fatigue crack growth life (and the development of the in-service inspection intervals), it is essential to have a detailed and reliable characterisation of the residual stress introduced in the material at the processed hole. Such knowledge is also required to improve the performance, reliability and repeatability of the SSCx<sup>TM</sup> process.

Many studies have been conducted to characterise the residual stress induced by SSCx<sup>TM</sup> process including numerical Finite Element (FE) modelling [6–8] and various experimental techniques, such as X-ray Diffraction (XRD) [9], Neutron Diffraction (ND) [10] and modified Sach's boring [11]. All measurement techniques have strengths and limitations, for example whilst XRD and ND are non-destructive, their spatial resolution is limited by the gauge size and by a large material grain size [12]. One major challenge for accurately determining the residual stress at Cx holes is the very steep residual stress gradient near the edge of the hole [10]. In addition to this, XRD can only determine surface stresses penetrating to a depth of tens of microns. Whilst ND can characterise stresses in samples up to 30–40 mm deep, the sample has to be taken to a central facility for access to an expensive high intensity reactor or pulse neutron source [10]. On the other hand, the Sach's boring technique is a relatively quick and cost effective laboratory measurement method, but the specimen cannot be reused, and it assumes a residual stress distribution that is uniform through the thickness [11, 13, 14], which has been demonstrated to limit the effectiveness of the characterised residual stress field in crack growth predictions [4, 15–18].

The contour method allows for the determination of residual stresses along a plane of interest. It was first proposed in [19], has also been applied to Cx hole components [20–22]. It has the unique advantage of being able to provide a two-dimensional map of residual stress across a plane of interest with relatively high spatial resolution. The technique involves cutting the component into two halves by wire Electro Discharging Machining (EDM) to relax the existing residual stress. Corresponding relaxed out-of-plane deformation on the cut surfaces of the two halves is accurately measured by a Coordinate Measurement Machine (CMM). The measured deformation contours of the cut faces are then averaged and smoothed to remove shear stress effects and noise respectively. Finally, the opposite sign of the averaged smoothed deformation data are applied as boundary conditions to a 3D linear elastic FE model of one cut half of the component to determine the pre-cut residual stress acting normal to the cut plane. The technique has been applied to many engineering components with different material and complex geometries [23–25] and extended to determine

different stress components using multiple cuts [26] and multiple methods [27]. The technique is described in detail in [28, 29].

The accuracy of the contour method critically depends on minimising the error sources, such as artefacts introduced by the EDM cutting process [28, 30] near surface uncertainties [31, 32], bulge [32] and Cutting-Induced Plasticity (CIP) [33, 34]. In this study we focus on CIP and its mitigation in the Cx plate application. Plasticity is a major source of residual stress determination error in Mechanical Strain Relaxation (MSR) techniques that rely on the assumption that the stress relaxation process is purely elastic. Unsurprisingly, CIP generally occurs near the region where the magnitude of residual stresses approaches the yield stress of the material [35, 36]. Extensive studies have been conducted by many research groups to understand and control stress redistribution plasticity during the cutting process for contour method measurements. One approach is to apply mechanical restraint (clamping) near the cut surface during wire EDM cutting [33, 37]. Another is to design a bespoke cutting path configuration that has been optimised using prior knowledge of residual stress field in the component [38, 39]. A third approach, with practical benefits, is to use self-restraint of the structure by starting the cut from a pilot hole located a few millimetres within the component of interest [12, 40, 41]. The latter strategy, often referred to as an “embedded cutting configuration”, was initially developed at The Open University. The concept is to use the stiffness of the structure to control the concentration of re-distributing stresses ahead of the wire EDM cut slot and thereby limiting plasticity and cut tip displacement errors. The stress field ahead of the cut tip is essentially characterised by the linear elastic Stress Intensity Factor (SIF); this provides a means for comparing the effectiveness of restraint strategies and the benefits of using a ‘single’ embedded cutting configuration [34]. The benefits of controlling the SIF by using 5 intermittent cuts 4 along the same plane has been demonstrated by Muránsky et al. [12]. Here it was shown that further improvements can be achieved by delaying the cut through the region of interest, if it contains significant internal stresses, until these stresses are relaxed via release of the equilibrating stresses found outside the region of interest. However, this double-embedded cutting strategy has been primarily implemented on weldments containing high tensile residual stress levels and its efficacy for other engineering components with different residual stress states is yet to be demonstrated.

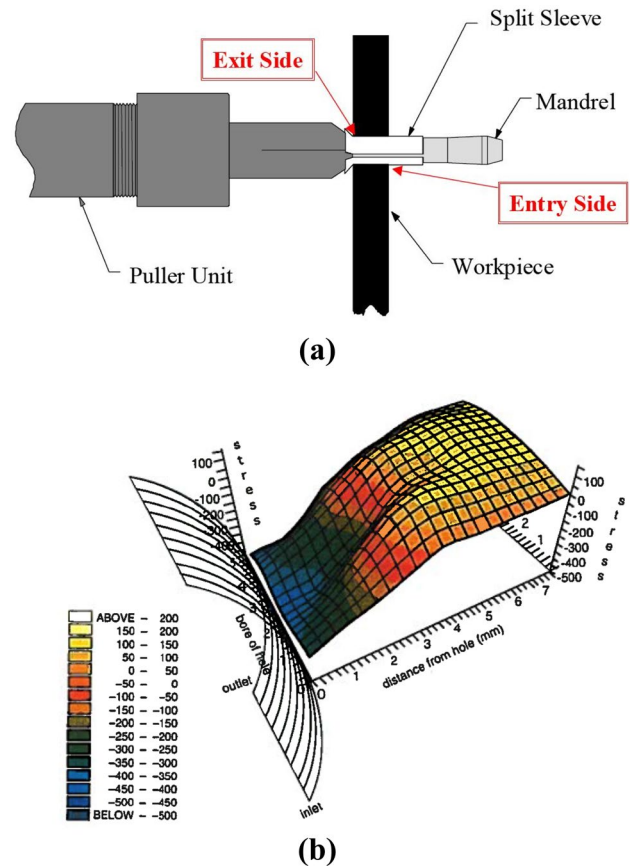
This paper examines the merits of applying different contour method cutting strategies for determining the residual stress distribution in a Cx hole test coupon. In order to investigate this a representative residual stress field is introduced into a 3D elastic-plastic FE analysis of the Cx test coupon. The simulated coupon is then cut in half to simulate the contour method. Through this process it is possible to predict

the residual stress state in the coupon for each of the contour cutting strategies. Details of the predicted magnitude, locations of plasticity and their effect on the apparent determined stress field are discussed. These predicted results are then compared with stress data from contour measurements of Cx hole test coupons to confirm the value and validity of the numerical simulation.

## Split Sleeve Cold Expansion (SSCx<sup>TM</sup>) Process and Test Components

The SSCx<sup>TM</sup> process is performed by hydraulically pulling a tapered mandrel through a lubricated sleeve that has been installed in the processed fastener hole. The combined maximum diameter of the mandrel and the sleeve is greater than the diameter of the hole such that as the mandrel is pulled through the hole, increasing radial interference plastically deforms the material surrounding the hole creating a plastically strained zone [5, 42]. This process produces an elastically strained region that can reach up to one diameter away from the hole. The displacement mismatch between these two strained regions produces a self-equilibrated residual stress field around the hole. High magnitude compressive residual stress in the hoop direction near the bore reduces and becomes tensile at around one radius away from the edge of the hole [43–45]. Figure 1(a) illustrates the SSCx<sup>TM</sup> process and Fig. 1(b) shows a typical residual stress field created by the SSCx<sup>TM</sup> process.

Three test coupons of dimensions of  $126 \times 100 \times 6$  mm<sup>3</sup> were made from Aluminium 2024-T351 plate, having a Young's modulus of 73,773 MPa and Poisson's ratio of 0.33 [46]. A 12.12 mm diameter hole was drilled at the centre of each coupon. The same SSCx<sup>TM</sup> process was applied to all three test coupons and all coupons were processed during the same processing session to minimise processing error. These coupons were designed to have a starting hole diameter that would allow for the introduction of a 3.16% applied expansion level. For this hole diameter the FTI spec allows for an applied expansion range between 3.16% to 4.16%. The goal for all of these coupons was to provide an applied expansion level which would be at the “low” end of the specification [47]. For all three of the test coupons the standard 16-0-N FTI tooling was used. For that tool set the max mandrel diameter was 11.8948 mm. The final diameter of the Cx processed hole was about 13 mm, see Fig. 2(a). The material stress-strain properties at room temperature were determined by Southwest Research Institute (SwRI) to ASTM E8 [48] using a 12.7 mm wide, 7.6 mm thick tensile specimen with a gauge length of 50.8 mm. Strain was measured using an extensometer and with strain gauges applied on each side of the specimen. The tensile test results are depicted in



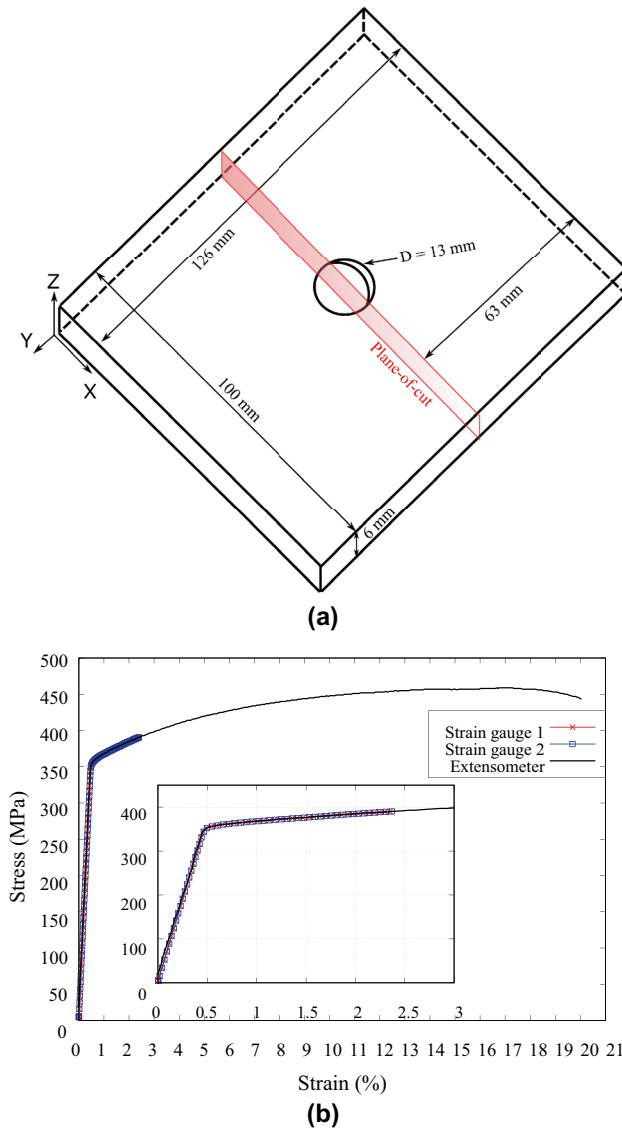
**Fig. 1** (a) FTI's SSCx<sup>TM</sup> set-up with mandrel, sleeve and workpiece shown – highlighting the entrance and exit side of the Cx process. Figure is from [16]. (b) Typical 3D residual stress distribution around a Cx hole, determined by neutron diffraction technique, Figure is from [10]

Fig. 2(b) and give a measured 0.2% proof stress of 359 MPa and UTS of 459 MPa at a final strain of 22%.

## Contour Method Simulation

FE simulations of the planned contour method were conducted first in order to study the stress re-distribution during cutting, the likely associated plastic deformation, and consequential stress determination errors. Three wire EDM cutting sequences were assessed with their corresponding boundary conditions in order to understand the mechanics and identify the approach that minimised predicted stress errors due to CIP in the regions of most interest (close to the Cx hole bore).

FE simulation of the contour method process involved the following steps: 1) introducing a residual stress field into a 3D FE model of the coupon similar to that created by the Cx process; 2) predicting the elastic-plastic redistribution of residual stress as the coupon was cut, taking account of the cutting pathway/sequence, material removed and applied



**Fig. 2** (a) A schematic diagram of the Cx hole test coupon, indicating that contour cut is performed at mid-length on a ZX plane along the Y axis. (b) Al2024-T351 stress-strain curve obtained from a tensile test. Two strain gauges were glued on each side of the specimen together with extensometer measurement. The number of points in the lines was reduced for clarity of the figure

boundary conditions; 3) extracting displacement contour data from the simulated cut surfaces; 4) applying this contour data set as a boundary condition to a separate FE model of the cut component and carrying out a linear elastic mechanical analysis to determine the simulated contour residual stress data; and 5) comparing this “measurement” with the original residual stress field introduced in step 1).

Three different cutting sequences were investigated: a) a single cut (referred as Edge-to-edge), starting from the left outer edge of the coupon and terminating at the right edge, after passing through the centre of the hole, see Fig. 3(a);

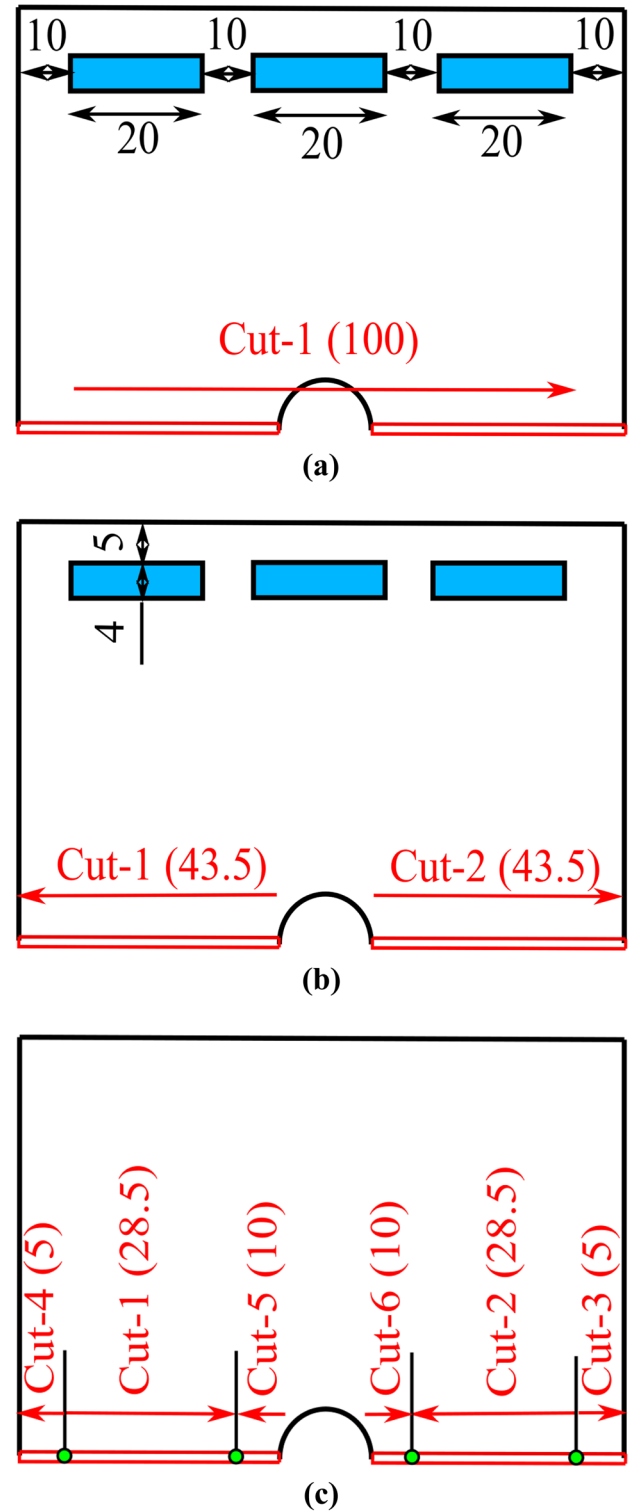


**Fig. 3** Schematics illustrating the different cutting sequences studied: (a) single straight cut, (b) two hole-out cuts, and (c) 6-cut cutting strategies. Blue regions in (a) and (b) are the areas over which restraint was applied to representing clamping strategy, and green circles in (c) indicate 1.8 mm diameter pilot holes for the 6-cut strategy. The numbers in the figures indicate the dimension in mm



b) two sequential cuts (referred as hole-out), each starting from the inner edge of the Cx hole, the first progressing to the left edge of the coupon and the second cut to the right edge, see Fig. 3(b); and c) a 6-cut sequence as illustrated in Fig. 3(c).

Two symmetry plane boundary conditions at  $Y = 0$  and  $Z = 0$  were applied allowing a one-quarter model to be used for the simulation studies, see Fig. 4. Cutting sequences a) and b) were simulated with surface nodes restrained within the blue regions depicted in Fig. 4(a). These boundary conditions, referred to as “Standard Restraint”, represent standard contour measurement practice where samples are clamped onto a baseplate on both sides of the planned cut line. Then cutting sequence (c) was simulated with low restraint (but effectively unrestrained) boundary conditions that just removed rigid-body motion. In this case restraint in the  $X$  direction was applied at the bottom centre node on the  $Z = 0$  plane, see Fig. 4(b). During the cutting simulation the  $Y$  and  $Z$  symmetry conditions restrained deformations acted in the  $Y$  and  $Z$  directions. However,  $Y$  symmetry condition was progressively released during the cutting simulation and therefore additional  $X$  and  $Y$  direction restraints were applied to the top centre node on the  $Z = 0$  plane right before completion of the cut, see Fig. 4(b).

Cutting sequence c) generally involved the introduction of two pilot holes (of diameter 1.8 mm) positioned 5 mm away from the outer edges of the coupon (where the magnitude of residual stresses were low). The first cut started from the left pilot hole and terminated at an intermediate pilot hole after cutting inwards 28.5 mm. A second cut was then performed in a mirror-symmetric manner starting from the right pilot hole. Next, the ligaments beyond the pilot holes on both sides of the specimen were severed in an outward direction. Finally cut-5 and cut-6 were used to cut the regions of most interest near to the inner surface of the Cx hole. The multi-cut approach uses the principal of “self-restraint” to limit plastic deformation associated with residual stress re-distribution as the coupon is cut. The specific sequence was designed to eliminate cutting plasticity in the region of interest near the bore and control CIP levels elsewhere during the cut. The optimum location of pilot holes relative to the edge of a sample has been studied previously [12] for welded components. If the distance is  $< 5$  mm, then there is a risk that the cut-opening self-restraint provided by the ligament is insufficient to limit the stress intensification ahead of the cut (and may result in local plastic deformation). On the other hand if the ligament is too long then relaxation of high magnitude stresses by partial cuts 1 and 2 may be insufficient. Likewise the 28.5 mm cut length was chosen to ensure sufficient relaxation of compressive residual stress near the Cx hole, whilst keeping stresses low enough to avoid CIP.

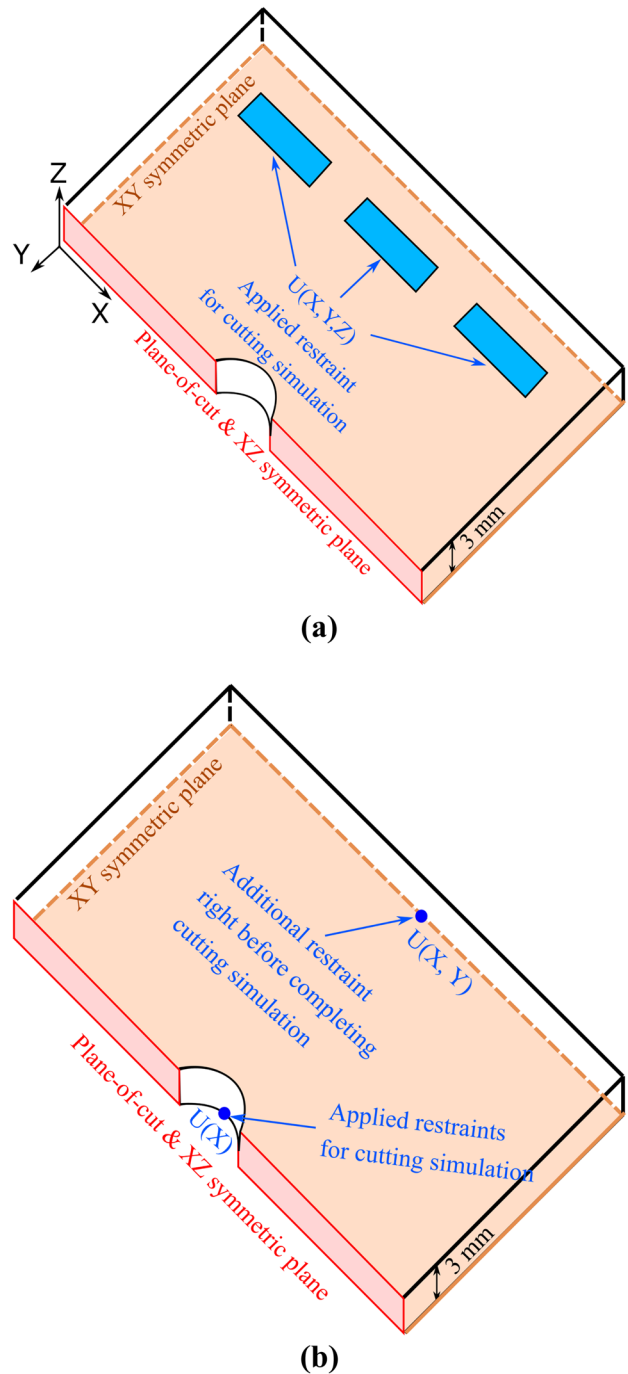


**Fig. 4** Schematic illustrations of two different boundary conditions for the FE cutting simulation: (a) “standard restraint” and (b) “unrestrained”

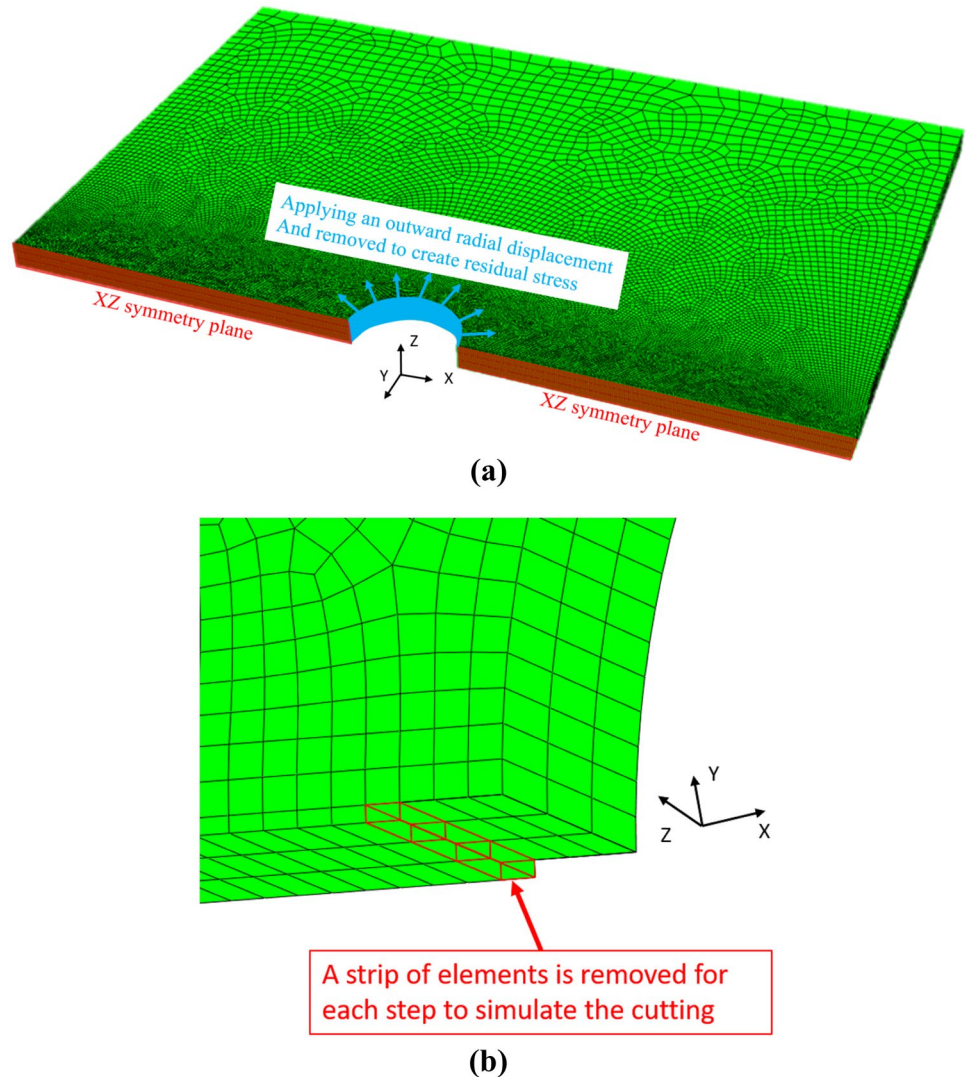
### Step 1: Create 3D FE Model of Coupon with Cx Residual Stress Field

The 3D FE model of the coupon was created (and analysed) using ABAQUS 6.13 software [49]. Two symmetry plane boundary conditions at  $Y = 0$  and  $Z = 0$  were applied

allowing a one-quarter model of the actual geometry of the coupon to be used for the simulation studies, see Fig. 5(a). A total of 81,546 four-node linear elements with reduced integration points were used. The elements belong to three families: elements approximately  $0.2 \times 0.1 \times 1 \text{ mm}^3$  to be removed in order to simulate the cutting process; elements approximately  $0.2 \times 0.2 \times 1 \text{ mm}^3$  in the immediate vicinity of the cut plane and near the hole; and the remaining elements biased from 0.2 to 2 mm along the  $Y$ -axis, see Fig. 5(a). The elements were assigned the material properties described in “Split Sleeve Cold Expansion (SSCx<sup>TM</sup>) Process and Test Components” for Al2024-T351 with an isotropic hardening assumption [50]. This simple hardening model was judged appropriate to represent to one-half elastic-plastic cycle associated with the Cx simulation and any subsequent half-cycle introduced by contour method stress re-distribution. For the purpose of optimising contour cutting strategies the contour method simulations used rate independent material properties.

The Cx process was simulated in a simplified way by applying an outward radial displacement of 0.195 mm (3% expansion) to the surface nodes of elements through the thickness of the bore in an elastic-plastic large-displacement finite element analysis, see Fig. 5(a). This applied displacement loading condition generated localised plastic deformation, corresponding to a 5.3% maximum equivalent plastic strain and an idealised residual stress field surrounding the hole with a peak compressive hoop stress of 462 MPa close to the hole edge when the applied displacement was removed, see Fig. 6. It should be noted that this work did not intend to simulate the details of the complicated SSCx<sup>TM</sup> process. Instead the purpose of contour method simulations was to implement a simplified modelling approach to generate a stress state in the coupons similar to those produced by the SSCx<sup>TM</sup> process and use this as a basis to understand how plasticity evolves as the coupons are cut for the contour method measurements and optimise the cutting strategy. Particularly, the amount of the applied radial displacement

**Fig. 5** (a) Schematic showing one quarter 3D FE model of the coupon with a Cx hole, and (b) close-up view of the mesh at the cutting plane. The modelled hole radius is 6.5 mm. An outward radial displacement of 0.195 mm was applied through the thickness of the bore of the hole and then removed to create an initial residual stress field



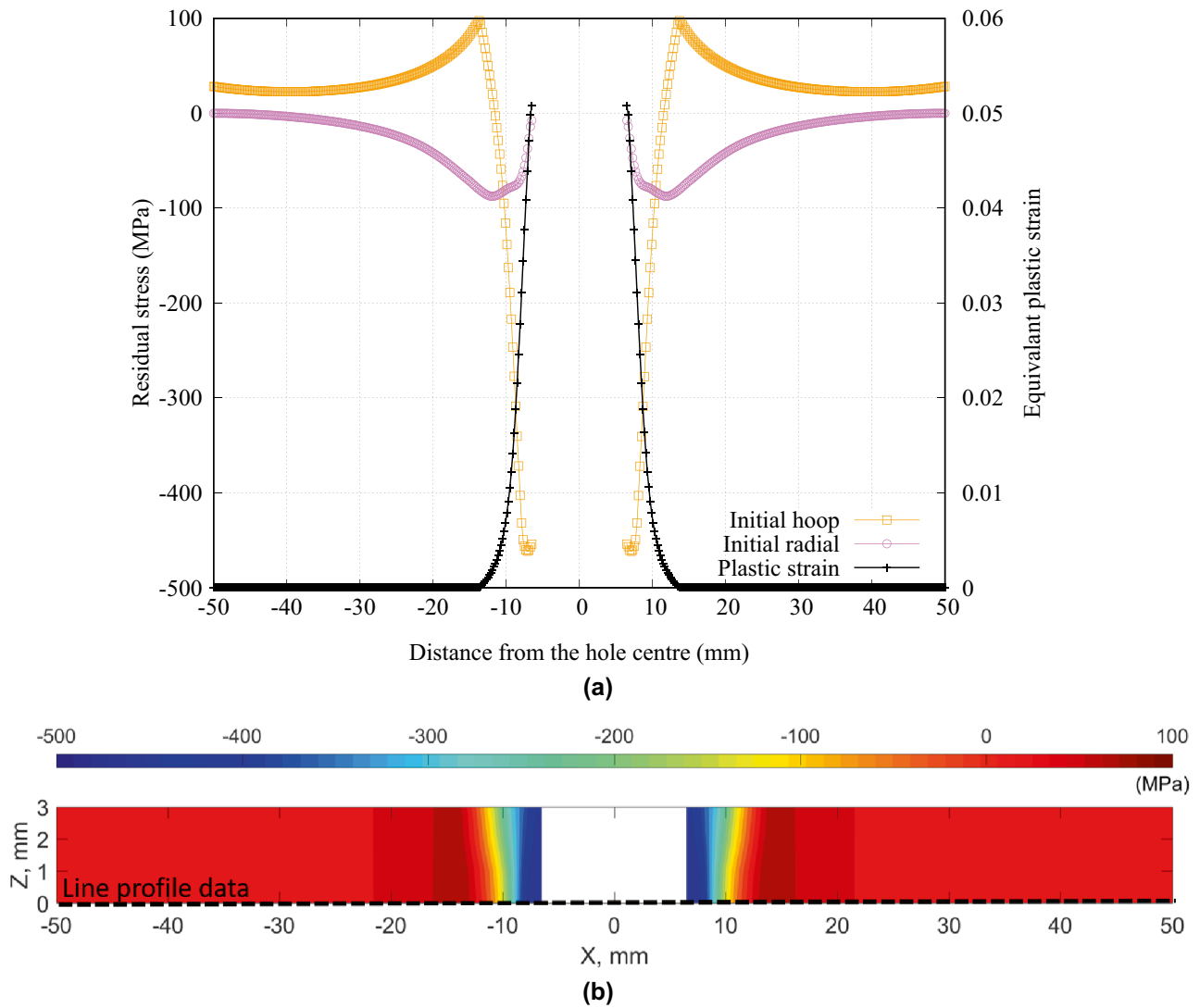


**Fig. 6** (a) The initial hoop and radial residual stress fields generated from a simulated Cx process, superimposed with induced equivalent plastic strain. The line profiles are obtained from the  $Z = 0$  ( $XY$  symmetry plane) along the  $X$ -direction. (b) Contour map illustrating

the distribution of hoop residual stress introduced by simulating the simplified cold expansion process. The maximum compressive hoop residual stress of 462 MPa is located near to the hole edge

in the FE simulation was on the basis of reaching the size of final hole diameter rather than implementing the actual expansion level in practice.

## Step 2: Contour Method Cutting Simulation

Following the simulation of the introduction of a representative residual stress field in the coupon model (and removal of the initial radial displacement at the hole), the “Standard Restraint” or “Unrestrained” boundary conditions, as shown in Fig. 4, were applied to the model as indicated in Fig. 5. Simulation of the wire EDM cutting process was simplified by incrementally removing through-thickness lines of three elements immediately ahead of the cut tip in an elastic-plastic mechanical analysis. No attempt was made to represent the

physics of the spark erosion process. The 0.1 mm width of cut elements represents a total resultant wire EDM cut width of 0.2 mm associated with a 0.15 mm diameter cutting wire, exploiting the symmetry boundary condition. The size of elements along the cut line determines the depth of each incremental step and is a critical parameter for this type of analysis [51]. The smaller the depth of cut at each step the more accurate the redistribution of residual stresses and the prediction of plasticity associated with progressive extension of the cut. However, increasing the number of cutting steps increases the computational time and a pragmatic choice of element size must be made. In the present case, cutting was simulated by progressively removing strips of three elements, each strip being 0.1 mm wide by 0.2 mm deep in the cutting direction and 3 mm wide in the through-thickness direction, see Fig. 5(b). Each of



the cutting sequences shown in Fig. 3 was modelled with one of the boundary conditions described earlier.

### Steps 3 and 4: Contour Method Simulation Back-Calculation

After the cutting simulation, out-of-plane displacements (in the  $Y$  direction) at the nodes of the cut faces were collected and applied as a boundary condition to corresponding nodes of a new FE model of the cut coupon and a linear elastic stress analysis was performed. Assuming elastic conditions have remained during cutting, and the loss of material is ignored, this procedure predicts the stress field in the component after relaxation has occurred due to the cutting. At the cut face the relaxed stress is equal to the residual stress that was acting normal to the cut plane in the original uncut component. This stress back-calculation procedure is conventionally used in the contour method with (processed) experimental cut face displacement data,

see “[Experimental Validation](#)”. However, the purpose of the contour cut simulation and present back-calculation was to identify the magnitude and distribution of the determined stress errors that can be introduced by the contour cutting process (and designed cutting sequence variants), that is by plasticity associated with stress re-distribution and relaxation as the cut progresses [32].

### Step 5: Assessment of Simulated Stress Measurement Error Results

Hoop residual stresses from the simulated contour method were calculated using the following cutting sequences (a) edge-to-edge, (b) hole-out with standard restraint and (c) 6-cut with unrestrained boundary conditions are compared with the initial hoop residual stress field in Fig. 7. Line profiles at  $Z = 0$  along the  $X$ -direction (on the  $XY$  symmetry plane) are presented in Fig. 8(a) with the region of particular interest (near the hole bore) highlighted. These results show

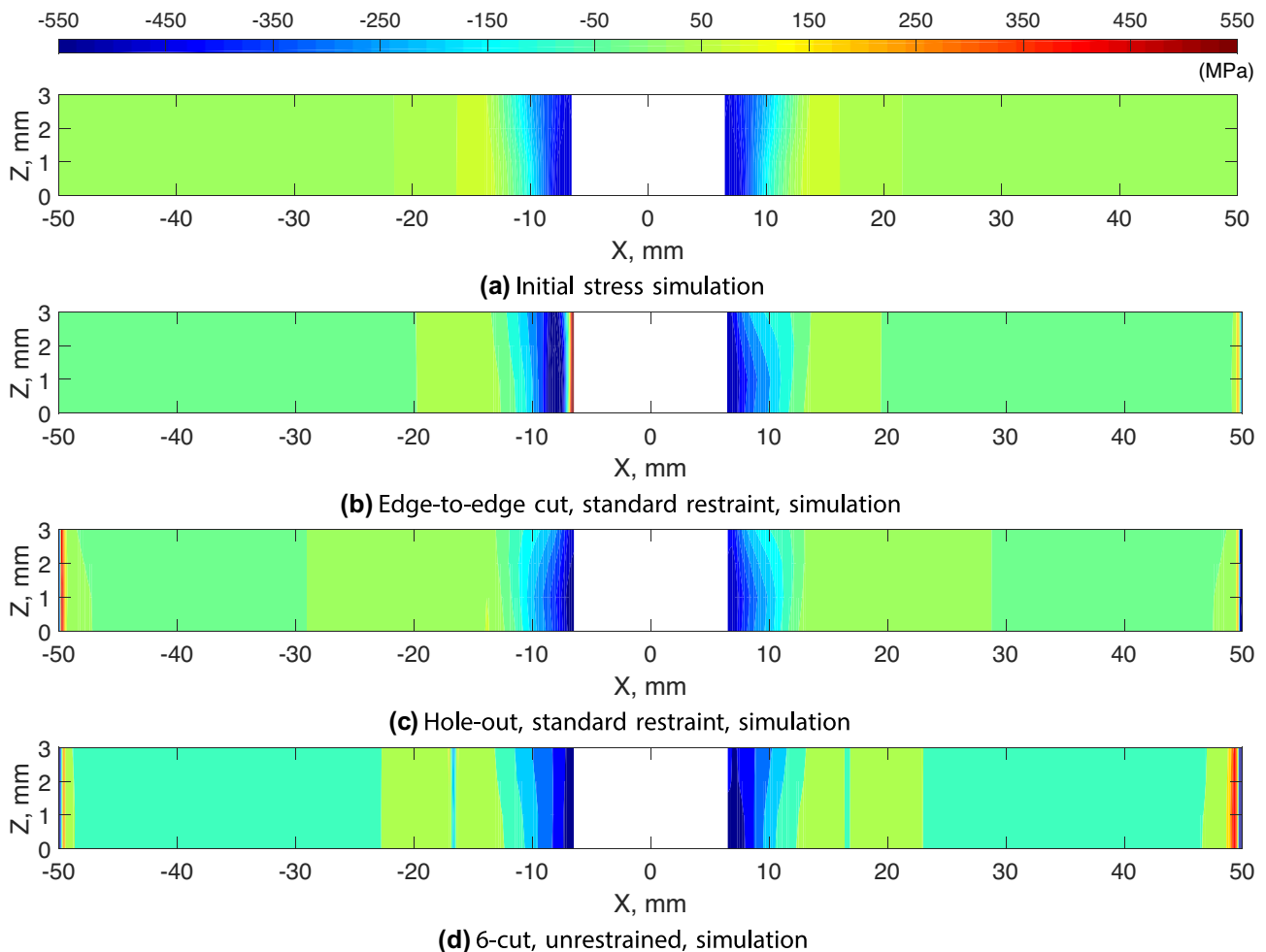
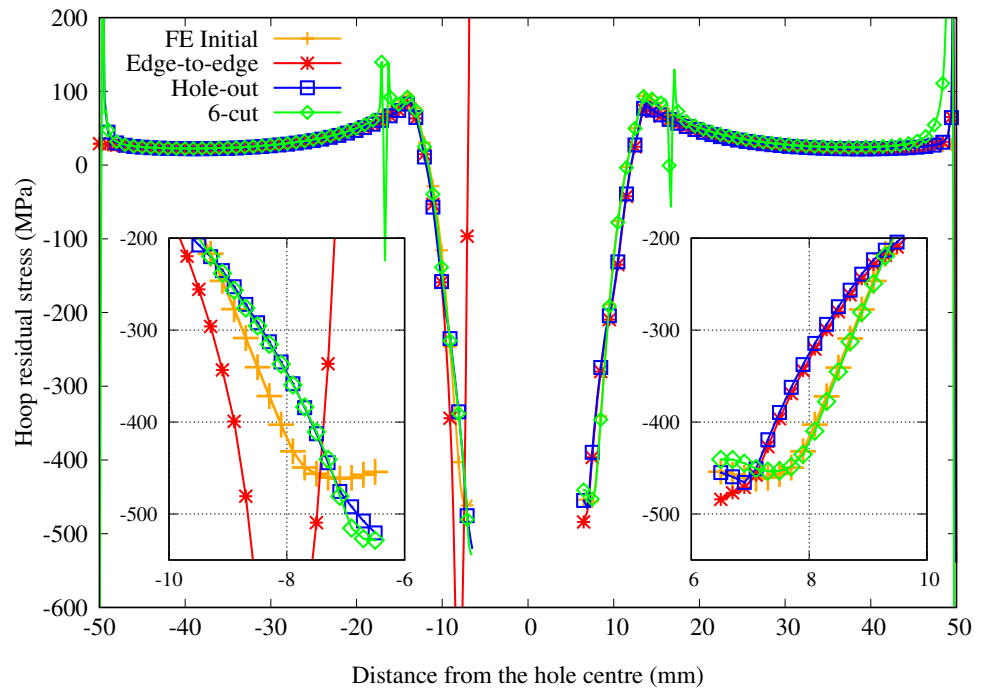


**Fig. 7** Predicted hoop residual stress maps from FE elastic-plastic simulated contour method measurements using different cutting sequences: (b) edge-to-edge, (c) hole-out, and (d) 6-cut, are compared with (a) initial residual stress field. Note (a) is the same stress map as presented in Fig. 6(b), but with a different contour scale

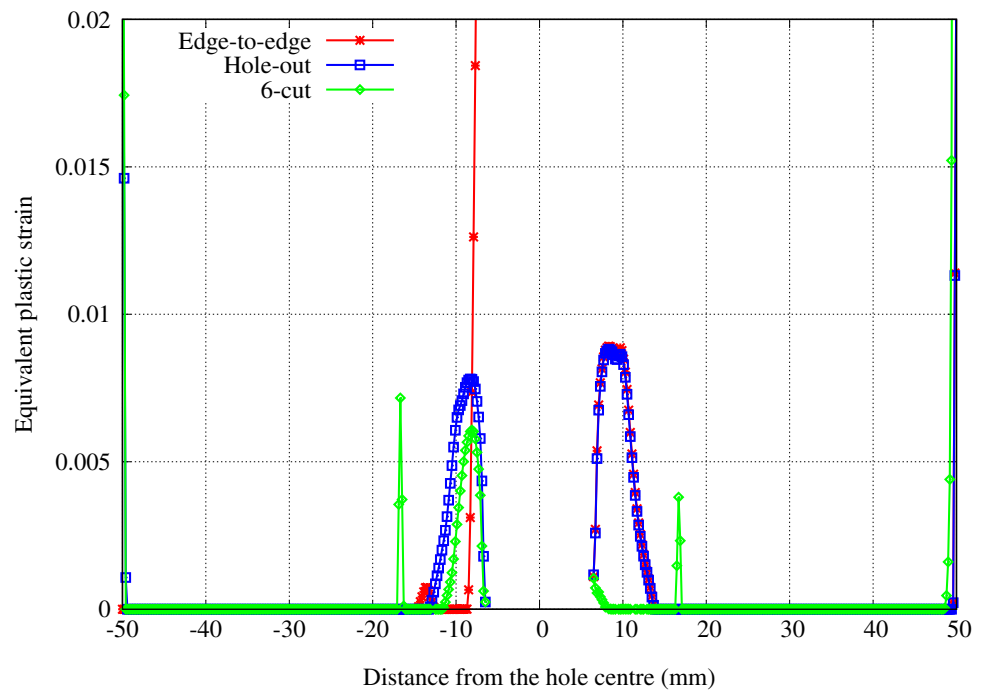
that the simulated residual stress profiles obtained from the hole-out and 6-cut cases generally give a much closer match to the initial FE predicted stress distribution than the edge-to-edge case, although in the 6-cut and hole-out cases there are localised stress spikes at the end of the coupon and the locations where cut-1 and cut-2 finish for the 6-cut strategy.

In particular, in the region of interest on the left side of the hole, a large stress error is evident in the edge-to-edge cut case. In the region of interest on the right side of the hole the residual stress distribution for all three cases are close to the initial FE predicted stress distribution, with the 6-cut case giving a near perfect match. It is also important to note

**Fig. 8** (a) Predicted hoop residual stress profiles at mid-thickness along the  $X$ -axis from the contour method simulations for different cutting sequences, compared with the initial residual stress field. (b) Predicted cutting induced plastic strain at the cut surface of the simulated contour method made using different cutting sequences and boundary conditions



(a)



(b)

in Fig. 8(a) that the shape and magnitudes of the stress profiles on the left and right side of the hole are not the same. These results show that the most accurate stress profile is obtained on the right side of the hole. This is because the remaining stresses on the right side of the hole during the cut is redistributed and relaxed by cutting the left side of the hole. For all of these simulations the right side of the hole was the last side to be cut, and thus it can be seen from these simulations that if a residual stress profile was to be picked for future analysis, the most accurate stress profile would be that developed from the last side of the cut through the hole.

It is instructive to inspect the predicted distributions of plastic strain introduced by the different cutting sequences. Figure 8(b) compares the predicted plastic strain (equivalent plastic strain output PEEQ in ABAQUS) on  $Z = 0$  along the X-axis of the cut surfaces. The plastic strain caused by the cutting simulation was obtained by subtracting the PEEQ output at the end of “Step 1: Create 3D FE Model of Coupon with Cx Residual Stress Field” from the PEEQ output at the end of the “Step 2: Contour Method Cutting Simulation”. As expected, the locations of stress error from the simulated contour method with the different cutting cases are consistent with those that have high magnitude equivalent plastic strain. There is an excessive plastic strain observed on the left side of the hole for the edge-to-edge case, while distributions of plastic strain of up to 1% magnitude extending radially outwards about 10 mm from the Cx bore were found on the right region of the hole for edge-to-edge and both regions for the hole-out cases. Whereas similar shape of distribution, but of lower magnitude occurred on the left region alone in the 6-cut case. The

significant reduction in CIP on the right side of the hole for the 6-cut case gives the stress profile that is in good agreement with the initial residual stress field. It can also be observed that, localised plasticity spikes are predicted where each cut exits the sample. These plastic strain errors cause local perturbations in the surface displacement field, which affect the back-calculated stresses, as shown in Figs. 7 and 8(a).

The impact of the accumulated CIP on the shape of stress field around the bore for each cutting strategy can be observed in Fig. 7. The predicted initial stress shows a steeper gradient in the X-direction in the mid-thickness of the sample ( $Z = 0$  mm) than in the top or bottom surfaces ( $Z = 3$  mm). This general behaviour is preserved by the 6-cut strategy whilst partly reversed for the edge-to-edge cut and fully reversed for the hole-out cut. For the edge-to-edge cut the CIP on the left side of the hole is very significant however very localised. This does not seem to have had impacts on the shape of the stress field. On the right side of the hole, the side that is cut last, the CIP is spread over a wider area and this has reversed the stress gradient along the X-direction. Similar observation on both sides of the hole can be seen for the hole-out cut. Controlling the CIP for the 6-cut strategy seem to have helped in preserving the expected stress field around the bore.

## Experimental Validation

The contour method was performed on samples with Cx holes in order to assess the validity of the FE study findings. Three coupons of dimensions  $126 \times 100 \times 6$  mm<sup>3</sup> with a single SSCx<sup>TM</sup>

**Fig. 9** Experimental set-up for the 6-cut cutting strategy showing the pilot holes and clamping arrangement

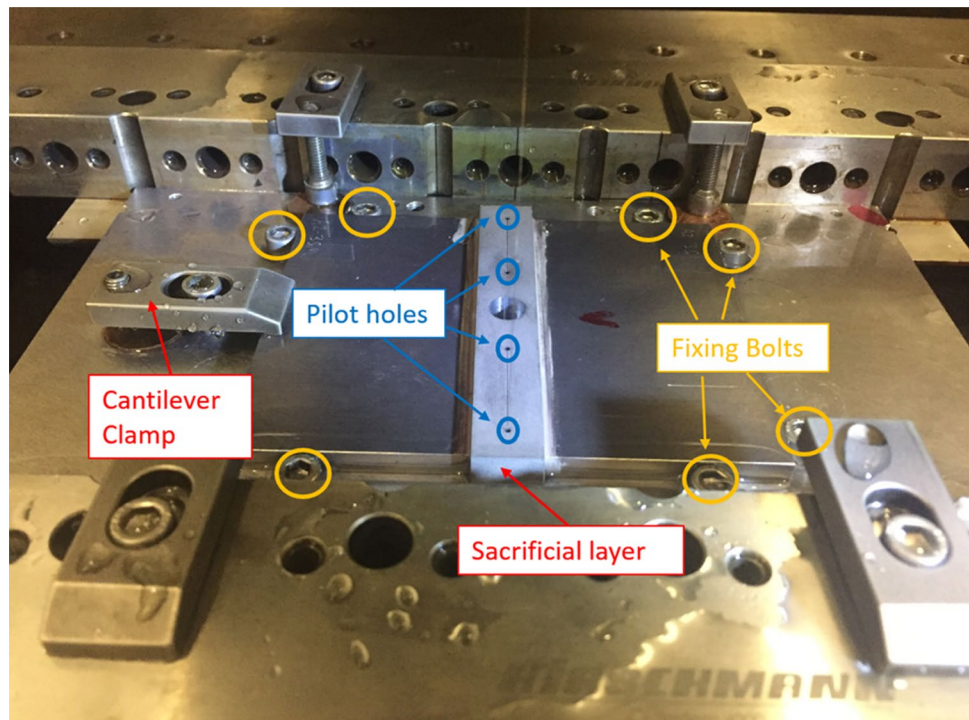


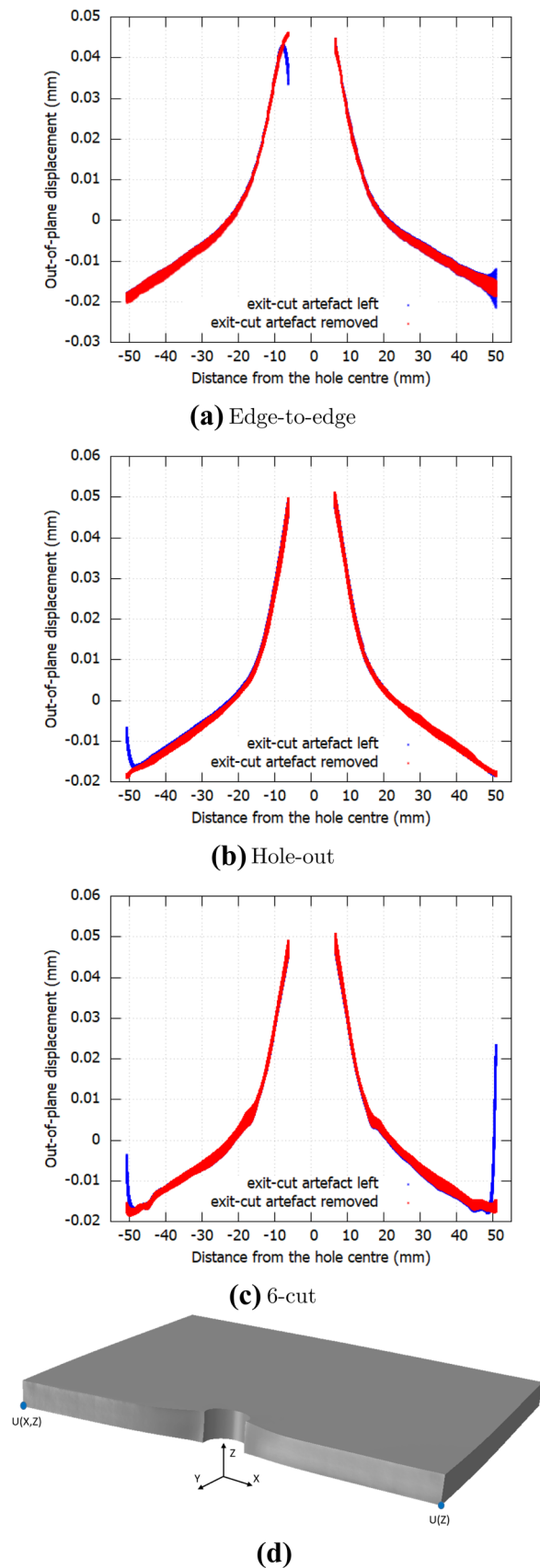
**Fig. 10** Processed out-of-plane displacement data with and without singularity error; (a) edge-to-edge, (b) hole-out, and (c) 6-cut cases. The opposite sign of processed displacement data were then applied to (d) the corresponding fully elastic FE model used to back calculate a 2D map of determined residual stress. Two additional boundary conditions were applied on bottom left and right corners of this elastic FE model to avoid rigid-body movement

processed hole in the middle of the coupon ( $R = 6.5$  mm) were manufactured from Al2024-T351 as described in “[Split Sleeve Cold Expansion \(SSCx™\) Process and Test Components](#)”. All of the contour cuts were made using an Agie Charmilles wire EDM machine (FI-440CS) with a 0.15 mm diameter wire. Sacrificial plate material [28, 31] was bonded to the top and bottom faces of each coupon using a conductive silver loaded epoxy glue in order to prevent through-thickness cutting artefacts associated with EDM wire entry and exit, see Fig. 9.

For the edge-to-edge and hole-out cutting sequences, each coupon was clamped at the locations simulated in the FE analysis, as shown in Fig. 4(a). To represent the unrestrained boundary condition for the 6-cut configuration, described in “[Contour Method Simulation](#)” and shown in Fig. 4(b), the two pilot holes of 1.8 mm diameter were drilled 5 mm away from the edges of the plates, as shown in see Fig. 9, and rigid body movement of the specimen during cutting was secured by 8 bolts fixed to the EDM bed around the four sides of the plate and a lightly forced cantilever clamp on the top face of the specimen. It is often the case that the EDM cutting wire cannot be rethreaded at the finish point of a prior cut owing to excessive cut face deformation (especially for a low stiffness aluminium alloy) and therefore two additional pilot holes were drilled where cut-1 and cut-2 finished.

The out-of-plane displacements of the cut surfaces were then measured using a Zeiss Eclipse CMM fitted with a Micro-Epsilon triangulating laser probe and a 4-mm diameter ruby-tipped Renishaw PH10M touch trigger probe. The touch trigger probe was used to measure the perimeter of the cut surface accurately and the triangulating laser probe was used to measure the relaxation displacements normal to the cut surface on a  $0.025 \times 0.025$  mm grid. The measured displacement data for each cut surface were then processed using the standard approach for contour measurement as described in “[Introduction](#)”.

Two different sets of processed displacement data were used in this study to assess the effect of local deviations in measured displacement on reconstruction of residual stress. The first dataset deliberately includes the measured local deviations in displacement at the edges of the coupon for comparison with the FE contour cut simulation studies; but displacement perturbations near the pilot hole regions from the 6-cut case were censored via the smoothing process, see Fig. 10(c). The second dataset censored all of the deviations and filled the gaps by interpolation or extrapolation. The two different sets of processed data from all cutting sequences are compared in Fig. 10.



Then, the processed displacement data from the three cut sequences were applied to FE models of the cut parts as boundary conditions, but with reversed sign. Additional restraints in  $X$  and  $Z$  directions in bottom left corner and  $X$  direction in bottom right corner of the model were applied to each model to stop rigid body motion, see Fig. 10(d).

## Experimental Results

Figure 11 shows the corresponding maps of determined hoop residual stress from the uncensored displacement data and Fig. 12(a) shows the line profiles at mid-thickness (at  $Z = 0$ ) along the  $X$ -direction. The hoop residual stress profiles are broadly consistent with the contour simulation, compare with Figs. 7 and 8(a). This gives us confidence in the validity

of the contour simulation study and its findings. The determined stresses from the hole-out and 6-cut cutting sequences agree with each other closely, with the maximum compressive hoop residual stress of about 450 MPa near the Cx hole bore, but the edge-to-edge cut gives a significantly different stress distribution approaching the left hand edge of the Cx hole. This change in the stress distribution was predicted by the FE process contour method simulation.

It is normal practice in conventional contour measurements to look critically at the measured displacement data and censor extreme outliers. This includes obvious artefacts like wire breaks and cut exit anomalies. The same displacement data were therefore processed to remove the cut exit stress singularity effects and extrapolate or interpolate and using a data smoothing algorithm across gaps in the displacement data, see Fig. 10. The back-calculation for each

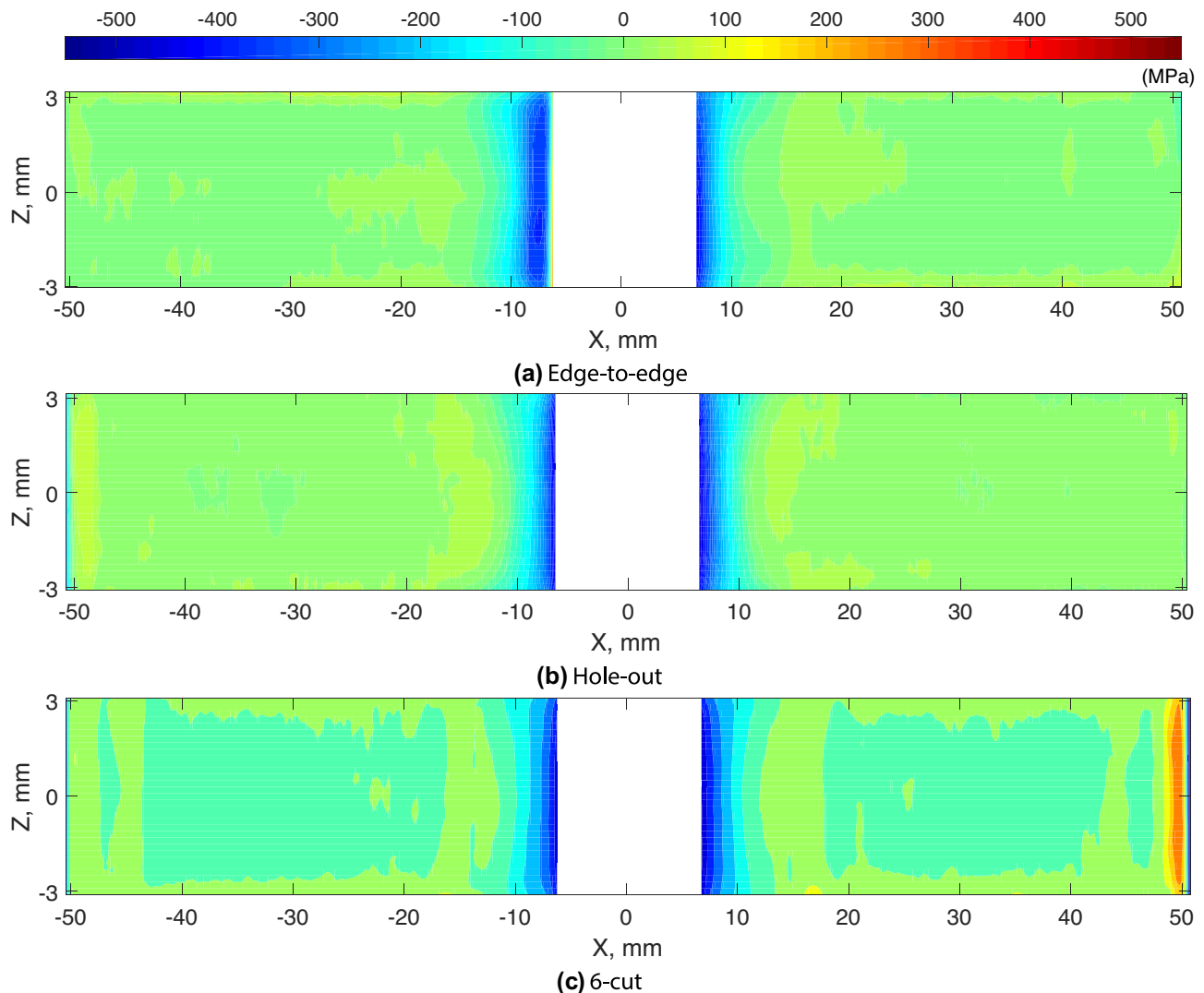


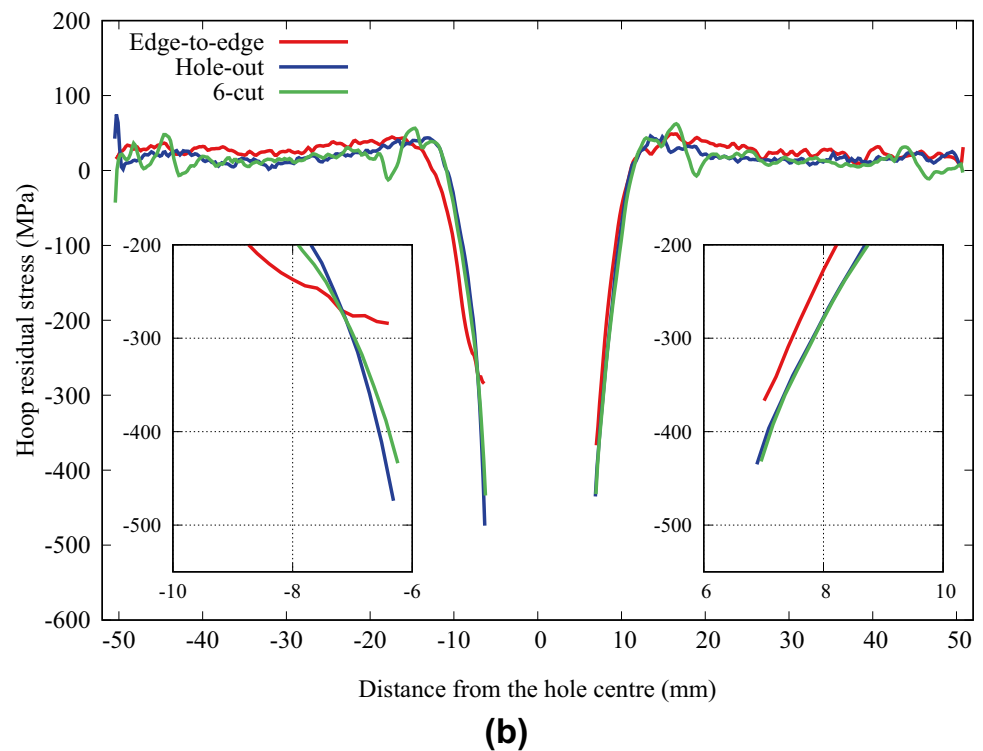
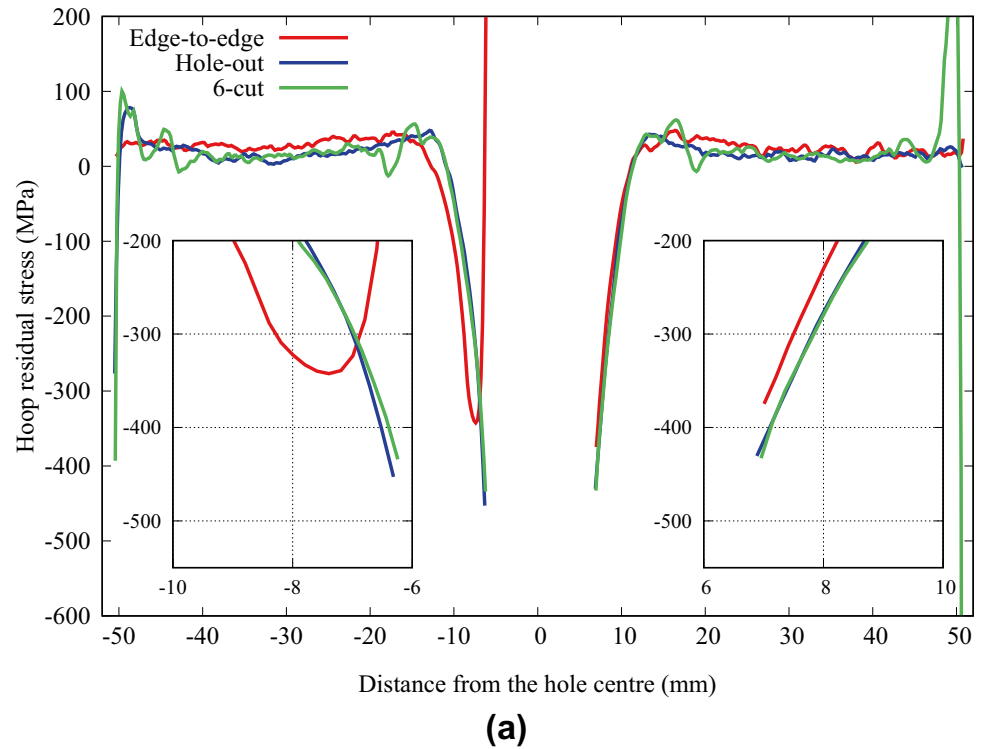
**Fig. 11** Determined hoop residual stress maps from different cutting cases: (a) edge-to-edge, (b) hole-out, and (c) 6-cut. The uncensored out-of-plane displacement data in Fig. 10 (blue dots) were used for stress back-calculation



sample was then repeated using the processed deformation data giving the residual stress results shown in Fig. 12(b). The stress profiles for the hole-out and 6-cut cases are similar to the results with the cut exit artefacts, except for both ends that have been corrected. But, the stress profile near the left side of the hole for the edge-to-edge cut (with cut

exit artefact removed) still deviates from the others, giving a hoop residual stress of about 170 MPa lower (compressive) magnitude than the 6-cut case at the bore. This result helps to verify the conclusions gain from the FE simulations, showing that the last side of the hole that is cut is the most accurate residual stress profile.

**Fig. 12** Determined hoop residual stress profile along the mid-thickness ( $Z = 0$ ) of the Cx coupons plates for different cutting cases: **(a)** with the uncensored and **(b)** censored out-of-plane displacement data, see Fig. 10



## Discussion

A rapidly varying residual stress field toward an edge, such as that approaching the edge of a Cx hole, is difficult to determine using the contour method [29]. A high quality wire EDM cut is required to provide accurate residual stress data. This requires many key elements which include a cut that is unperturbed by the stability of the wire cutting process [30], wire travel entry and exit effects [28] and stress re-distribution plasticity. Thus, it is often the case that contour stress results up to 0.5 mm from the surface edges are not reported because of wire travel entry and exit cutting artefacts unless special care has been taken to minimise this source of error [28, 31]. In the present experimental work, sacrificial material was bonded to the exposed top and bottom surfaces of the coupon to minimise surface proximity cutting artefacts. Sacrificial material was also bonded to the edges of the coupon, including inside of the Cx hole. This was done to help mitigate cut start-up transient conditions and changes in cutting conditions as the wire exited the coupon [28].

The present work has highlighted an additional important artefact that occurs when the cut exits an edge of the sample of interest. As the ligament length reduces, re-distributing stresses ahead of the cut can increase in magnitude and cause very localised plasticity that results in near edge displacement artefacts. These displacement artefacts are commonly removed and surrounding data is used to interpolated or extrapolated to the edges of the part or coupon. Reconstruction of the data across a gap in data within the interior of a specimen normally works very well, as demonstrated by the 6-cut case, see Figs. 10(c) and 12. However, extrapolation of interior data towards the edges of a specimen is less constrained and accurate results depend on the analyst's judgement regarding the local trend and what data they think should be included or discarded. Figure 12(b) clearly shows that the magnitude of the determined compressive stress near the left edge of the Cx hole, where data were extrapolated, is significantly lower than the stresses determined by the other cutting strategies. The lesson here is to choose a cutting strategy that avoids plastic strain accumulation near the region of interest, and thereby avoid subjective intervention.

The prediction of localised plasticity introduced by cutting the sample is of particular value in developing an optimum restraining and cutting approach. For the Cx coupon it was shown from the simulation that a near perfect contour measurement of the stress distribution on the right side of the hole (or last cut through the hole) can be achieved using a 6-cut approach. Therefore the actual stress profile determined by the 6-cut approach in the real sample is likely to be the most accurate result, particularly on the right side. This lesson is vital for the user of the residual stress data developed by the contour method. In the past it has been common practice to

average the data from the two sides of the hole. Through this work it has been demonstrated that accurate residual stress results depend on the cutting strategy and may be present on only one side of the hole. This must be communicated to the end user of this type of residual stress data to ensure that the most accurate residual stress data is used for predictions of crack growth life and continued structural integrity.

However, the experimental results indicates that in practice the difference between the hole-out and 6-cut approach was negligible. The difference between simulation and experimental results might be due to the limitations of the simulation work. First, the complex Cx process was simplified in the simulation by using an initial uniform expansion, whereas in practice a mandrel is pulled through the coupon which will give a varying residual stress field through the thickness. Beside, time-dependent visco-plastic behaviour of the material was ignored in the FE simulation. Secondly, the simulated cutting process does not represent the actual electro-discharge erosion process. The simulated cutting process was carried out by simply incremental removal of a layer of elements. Any loss of material and deformation on the cut surface due to the complex EDM process except the diameter of the EDM wire was ignored. Thirdly, the restraint applied in the FE simulation is idealised as rigid whereas in practice the restraint will be more compliant. Nevertheless the results from this study show that the residual stress results for the Cx holes that were investigated in this work are more accurate on the side of the hole where the last cut was made.

Plasticity for the 6-cut case was minimised by introducing pilot holes and using multiple cut paths. The first cut starts in a region of low magnitude residual stress and terminates before it reaches a high stress area. The use of ligaments in the 6-cut case acts to reduce stress intensification at the cut tip. In the case of the Cx hole, the high compressive stress region of particular interest was deliberately cut at the end. The main experimental drawback of the 6-cut approach is the need to machine pilot holes and carry out 6 cuts instead of 2 cuts. Additional data processing may be required to interpolate across displacement data gaps and deal with potential misalignment of the cut faces. These factors can lead to higher measurement uncertainty. Designing a suitable cutting strategy for minimising plasticity stress error is not a straight-forward process. It requires prior knowledge of the magnitude and the shape of imposed engineered residual stress field and the state of the yield surface prior to the contour cut. The present work has demonstrated that detailed FE simulation analysis can be a very effective tool in supporting the development of an optimum cutting sequence and in making correct choices of boundary conditions. Through optimizing these key aspects of the cutting sequence one is much more likely to have a successful, low error contour residual stress result.

## Conclusions

The SSCx<sup>TM</sup> process introduces a compressive hoop residual stresses of high magnitude around the hole. A more accurate distribution of residual stress along a radial line moving out from the Cx bore can be determined using the contour method with minimising error associated with CIP by carefully choosing contour cutting sequences. A 3D, non-linear FE simulation of the contour method as it would be performed on a Cx hole coupon was used to assess three different cutting sequences: edge-to-edge, hole-out, and 6-cut and determine which minimised plasticity stress errors near the Cx hole bore. The FE simulation shows that the location of the stress error is consistent with the location where CIP accumulated. The predicted shape and magnitudes of the stress profiles for all the cutting strategies are in better agreement with the initial stress prediction on the side of the hole where the last cut was made. It is, however, observed that the 6-cut approach that controls CIP gives the most accurate near bore stress result. In order to validate this hypothesis a high-quality contour measurement was performed. The empirical result showed that the hole-out cut which is experimentally simpler to implement than the 6-cut strategy provides indistinguishable result on the latter cut side of the hole where there is less likelihood of CIP. The experimental contour residual stress results on Cx hole coupons using three cutting sequences support the validity of the 3D FE contour residual stress simulation work.

**Acknowledgements** Manufacture of the Cx coupons was funded by the United States Air Force's A-10 ASIP Analysis Group out of Hill AFB, UT, USA. The coupons were machined and Cx holes were processed at the Southwest Research Institute (SwRI) in San Antonio, TX, USA. The measurement work was carried out at The Open University with help from StressMap and Technician Pete Ledgard. The UK authors gratefully acknowledge support for the Cx coupons research project from The Open University and Stress-Space Ltd. Dr. Foroogh Hosseinzadeh is grateful for support from EPSRC Grant EP/M018849/1.

## Declarations

**Conflicts of Interest** The authors have no conflicts of interest to declare that are relevant to the content of this article.

**Open Access** This article is licensed under a Creative Commons Attribution 4.0 International License, which permits use, sharing, adaptation, distribution and reproduction in any medium or format, as long as you give appropriate credit to the original author(s) and the source, provide a link to the Creative Commons licence, and indicate if changes were made. The images or other third party material in this article are included in the article's Creative Commons licence, unless indicated otherwise in a credit line to the material. If material is not included in the article's Creative Commons licence and your intended use is not permitted by statutory regulation or exceeds the permitted use, you will need to obtain permission directly from the copyright holder. To view a copy of this licence, visit <http://creativecommons.org/licenses/by/4.0/>.

## References

1. Finney JM (1993) Cold Expansion and Interference for Extending the Fatigue Life of Multi-Layer Metal Joints. Research Report 17 (AR-008-369), Defence Science and Technology Organisation, Aeronautical Research Laboratories, Melbourne, Australia
2. Phillips JL (1974) Sleeve coldworking fastener holes, volume 1. AFML-TR-74-10, Air Force Materials Lab, Wright-Patterson AFB OH
3. Ball DL, Lowry DR (1998) Experimental investigation on the effects of cold expansion of fastener holes. *Fatigue Fract Eng Mater Struct* 21(1):17–34
4. Chandawanich N, Sharpe WN (1979) An experimental study of fatigue crack initiation and growth from coldworked holes. *Eng Fract Mech* 11(4):609–620
5. McClung RC (2007) A literature survey on the stability and significance of residual stresses during fatigue. *Fatigue Fract Eng Mater Struct* 30(3):173–205
6. Chakherlou TN, Vogwell J (2004) A novel method of cold expansion which creates near-uniform compressive tangential residual stress around a fastener hole. *Fatigue Fract Eng Mater Struct* 27(5):343–351
7. Pavier MJ, Poussard CGC, Smith DJ (1999) Effect of residual stress around cold worked holes on fracture under superimposed mechanical load. *Eng Fract Mech* 63(6):751–773
8. Ribeiro RL, Hill MR (2017) Residual stress from cold expansion of fastener holes: Measurement, eigenstrain, and process finite element modeling. *J Eng Mater Technol* 139(4):07
9. Stefanescu D (2004) Measurement and prediction of fatigue crack growth from cold expanded holes part 1: The effect of fatigue crack growth on cold expansion residual stresses. *J Strain Anal Eng Des* 39(1):25–38
10. Wang D, Edwards L (1998) Neutron diffraction determination of the complete 3D residual stress distribution surrounding a cold expanded hole. In S. Denis, editor, 4<sup>th</sup> European Conference on Residual Stresses, ECRS-4, pages 619–626, Cluny en Bourgogne, France
11. Ozdemir AT, Edwards L (2004) Through-thickness residual stress distribution after the cold expansion of fastener holes and its effect on fracturing. *J Eng Mater Technol* 126(1):129–135
12. Muránsky O, Hosseinzadeh F, Hamelin C, Traore Y, Bendeich P (2018) Investigating optimal cutting configurations for the contour method of weld residual stress measurement. *Int J Press Vessel Pip* 164:55–67
13. Garcia-Granada AA, Smith DJ, Pavier MJ (2000) A new procedure based on Sachs' boring for measuring non-axisymmetric residual stresses. *Int J Mech Sci* 42(6):1027–1047
14. Smith DJ, Poussard CGC, Pavier MJ (1998) An assessment of the sachs method for measuring residual stresses in cold worked fastener holes. *J Strain Anal Eng Des* 33(4):263–274
15. Carlson S (2018) Quantifying the Effect of a Fatigue Crack on the Residual Stress Field Induced by the Split Sleeve Cold Expansion Process in 2024-T351 and 7075-T651 Aluminum Alloys. PhD thesis, University of Utah, Salt Lake City, USA
16. Carlson S, Pilarczyk T (2018) Using a beta ( $\beta$ ) correction to improve the life predictions of cold-expanded holes in 2024-T3 & 7075-T6 aluminum alloys. *Mater Perform Charac* 7(4):779–806
17. Chang JB (1977) Prediction of Fatigue Crack Growth at Cold-Worked Fastener Holes. *J Aircr* 14(9):903–908
18. Kokaly M, Ransom J, Restis J, Reid L (2005) Predicting fatigue crack growth in the residual stress field of a cold worked hole. *J ASTM Int* 2(5):1–13
19. Prime MB (2001) Cross-sectional mapping of residual stresses by measuring the surface contour after a cut. *J Eng Mater Technol* 123(2):162–168
20. Ismonov S, Daniewicz SR, Newman JC, Jr., Hill MR, Urban MR (2009) Three dimensional finite element analysis of a split-sleeve cold expansion process. *J Eng Mater Technol* 131(3)

21. Mills TB, Honeycutt KT, Prost-Domasky SA, Brooks CL (2015) Integrating Residual Stress Analysis of Critical Fastener Holes into USAF Depot Maintenance. Report Number A3G-2015-185420, Air Force Life Cycle Management Center, Hill AFB, USA
22. Zhang Y, Fitzpatrick ME, Edwards L (2002) Measurement of the residual stresses around a cold expanded hole in an EN8 steel plate using the contour method. *Mater Sci Forum* 404:527–534
23. DeWald AT, Hill MR, Willis E (2011) Measurement of Welding Residual Stress in Dissimilar Metal Welds Using the Contour Method. In ASME2011 Pressure Vessels and Piping Conference, volume 6: Materials and Fabrication, Parts A and B, pages 1599–1605, Baltimore, Maryland, USA
24. Hosseinzadeh F, Bouchard PJ (2013) Mapping multiple components of the residual stress tensor in a large P91 steel pipe girth weld using a single contour cut. *Exp Mech* 53(2):171–181
25. Kelleher J, Prime MB, Buttle D, Mummery PM, Webster PJ, Shackleton J, Withers PJ (2003) The measurement of residual stress in railway rails by diffraction and other methods. *J Neutron Res* 11(4):187–193
26. Pagliaro P, Prime MB, Swenson H, Zuccarello B (2010) Measuring Multiple Residual-Stress Components using the Contour Method and Multiple Cuts. *Exp Mech* 50(2):187–194
27. Pagliaro P, Prime MB, Robinson JS, Clausen B, Swenson H, Steinzig M, Zuccarello B (2011) Measuring inaccessible residual stresses using multiple methods and superposition. *Exp Mech* 51(7):1123–1134
28. Hosseinzadeh F, Kowal J, Bouchard PJ (2014) Towards good practice guidelines for the contour method of residual stress measurement. *J Eng* 2014(8):453–468
29. Prime MB, DeWald AT (2013) The Contour Method. In G. S. Schajer, editor, *Practical Residual Stress Measurement Methods*, pp 109–135
30. Bouchard P, Ledgard P, Hiller S, Hosseinzadeh F (2012) Making the cut for the contour method. In 15<sup>th</sup> International Conference on Experimental Mechanics, Porto, Portugal
31. Hosseinzadeh F, Ledgard P, Bouchard PJ (2013) Controlling the Cut in Contour Residual Stress Measurements of Electron Beam Welded Ti-6Al-4V Alloy Plates. *Exp Mech* 53(5):829–839
32. Prime MB, Kastengren AL (2011) The contour method cutting assumption: Error minimization and correction. In: Proulx T (ed) *Experimental and Applied Mechanics*, vol 6. Springer, New York, NY, pp 233–250
33. Shin SH (2005) FEM analysis of plasticity-induced error on measurement of welding residual stress by the contour method. *J Mech Sci Technol* 19(10):1885–1890
34. Traoré Y, Hosseinzadeh F, Bouchard PJ (2014) Plasticity in the Contour Method of Residual Stress Measurement. *Adv Mater Res* 996:337–342
35. Beghini M, Bertini L, Raffaelli P (1994) Numerical-analysis of plasticity effects in the hole-drilling residual-stress measurement. *J Test Eval* 22(6):522–529
36. Lin YC, Chou CP (1995) Error induced by local yielding around hole in hole drilling method for measuring residual stress of materials. *Mater Sci Technol* 11(6):600–604
37. Prime MB, Gnaupel-Herold T, Baumann JA, Lederich RJ, Bowden DM, Sebring RJ (2006) Residual stress measurements in a thick, dissimilar aluminum alloy friction stir weld. *Acta Mater* 54(15):4013–4021
38. Kim HK, Coules HE, Pavier MJ, Shterenlikht A (2015) Measurement of Highly Non-Uniform Residual Stress Fields with Reduced Plastic Error. *Exp Mech* 55(7):1211–1224
39. Kim HK, Shterenlikht A, Pavier MJ, Velichko A, Alexander NA (2016) On stability of a new side cut destructive method for measuring non-uniform residual stress in thin plates. *Int J Solids Struct* 100–101:223–233
40. Hosseinzadeh F, Traore Y, Bouchard PJ, Muránsky O (2016) Mitigating cutting-induced plasticity in the contour method, part 1: Experimental. *Int J Solids Struct* 94:247–253
41. Muránsky O, Hamelin CJ, Hosseinzadeh F, Prime MB (2016) Mitigating cutting-induced plasticity in the contour method. Part 2: Numerical analysis. *Int J Solids Struct* 94:254–262
42. Rufin AC (1993) Extending the fatigue life of aircraft engine components by hole cold expansion technology. *J Eng Gas Turbines Power* 115(1):165–171
43. Armen H, Levy A, Eidinoff HL (1984) Elastic-plastic behavior of coldworked holes. *J Aircr* 21(3):193–201
44. Ball DL (1995) Elastic-plastic stress analysis of cold expanded fastener holes. *Fatigue Fract Eng Mater Struct* 18(1):47–63
45. Sha GT, Cowles BA, Fowler RL (1980) Fatigue Life of a Coldworked hole. In *Emerging Technologies in Aerospace Structures, Design, Structural Dynamics and Materials, The Aerospace Conference - Centry 2 - Emerging Technology Conference*, pages 125–140, San Francisco, USA
46. Institute Battelle Memorial (2011) *Metallic Materials Properties Development and Standardization*. Report Number MMPDS-06, Columbus, USA
47. Fatigue Technologies Inc (2002) FTI Process Specification 8101D Cold Expansion of Holes Using the Standard Split Sleeve System and Countersink Cold Expansion (CsCx<sup>TM</sup>). Technical report, Seattle, WA, USA
48. ASTM E8 / E8M-16ae1 (2016) *Standard Test Methods for Tension Testing of Metallic Materials*. West Conshohocken, PA
49. Dassault Systèmes Simulia Corp (2013) *Abaqus Analysis User's Guide*, Version 6.13. Providence, RI, USA
50. Guillaume R, Gang L (2019) Plasticity Modeling for Hole Cold Expansion Residual Stress Prediction. In *Holistic Structural Integrity Process (HOLSIP) Workshop*, Salt Lake City, Utah, USA
51. Traoré Y (2013) Controlling plasticity in the contour method of residual stress measurement. PhD thesis, The Open University, Milton Keynes, UK

**Publisher's Note** Springer Nature remains neutral with regard to jurisdictional claims in published maps and institutional affiliations.

